RSC Advances

PAPER

View Article Online
View Journal | View Issue



Cite this: *RSC Adv.*, 2020, **10**, 7635

# Enhancement and mechanism of vermiculite thermal expansion modified by sodium ions

Jinpeng Feng,* Meng Liu, Linzong Fu, Kan Zhang, Zhenhui Xie, Dawei Shi and Xin Ma

Received 9th January 2020
Accepted 4th February 2020

DOI: 10.1039/d0ra00223b

rsc.li/rsc-advances

Aimed at improving vermiculite's thermal expansibility, a novel method of $Na^+$ modification has been proposed. The modification effects were characterized *via* X-ray fluorescence spectroscopy, X-ray diffraction, and thermogravimetric-differential thermal analysis. The result indicated that sodium ions entered vermiculite interlayers through the exchange of interlamellar calcium ions. The effects of the heating time on the expansion ratio of Raw-V and Na-V samples were investigated at the temperature range of 400–700 °C. The result indicated that the maximum increment in the expansion ratio could reach up to 26.5% after $Na^+$ modification. The influencing mechanism of $Na^+$ modification on the thermal expansibility of vermiculite was explored *via* molecular dynamics simulation and the binding energy and dehydration enthalpy change calculation. The simulation and calculation results showed a good agreement with the expansion experiment result. This study provides a novel method for the preparation of high-performance expanded vermiculite.



## 1. Introduction

Nowadays, the world is facing increasing serious energy and environmental problems because the demand for energy is increasing significantly, driven by the increases in prosperity in developing countries. In the global energy consumption system, fossil fuels, such as oil, coal, and natural gas, are playing a dominant role. Undoubtedly, the emission of pollutants from fossil fuel combustion to the atmosphere causes a variety of negative impacts on the climate and air quality. Therefore, the global energy system faces a dual challenge: the need to meet the rising energy demand while reducing the carbon emission simultaneously.[1–3] Thus, research on how to reduce energy consumption and improve energy efficiency has become a hot-spot. Developing high performance thermal insulating materials is considered as a potential method for solving energy and environment problems.

Vermiculite is a multilayer silicate mineral mainly consisting of hydrated silicate of magnesium, aluminium, iron, calcium and potassium. Due to the multiple action of natural weathering, hydrothermal action, and percolating ground waters in geological processes, vermiculite is formed with a layered structure containing plenty of interlayer water.[4–6] When heated during a short period of time, vermiculite can rapidly expand or exfoliate many times its original thickness because of the interlaminar water vapour pressure.[7,8] Because of numerous excellent properties, such as low density, low thermal conductivity, high temperature resistance, and high thermal stability, expanded vermiculite is usually used as a thermal insulating material.[9–11] In general, the thermal insulating performance of expanded vermiculite is closely related to the expansibility. Many studies were carried out to investigate the behaviors of vermiculite's thermal expansion.[12,13] Justo *et al.* suggested that the sudden release of interlayer water is not the only factor influencing the vermiculite's thermal expansion, *i.e.*, the presence of relicts of altered mica, loss of OH groups or the chemical composition can also affect the thermal expansion.[14] Marcos *et al.* found that a higher expansion was achieved in the case of mixed-layer vermiculite-mica minerals or mixed-layer vermiculite minerals containing vermiculite in different hydration states.[15–17]

In this study, aimed at improving the thermal expansibility of vermiculite, a novel method of $Na^+$ modification was proposed, and a thermal expansion experiment was conducted to investigate the effects of the heating temperature and time on the expansion ratio. Moreover, the molecular dynamics simulation combined with the calculation of binding energy (BE) and dehydration enthalpy change ($\Delta H$) was used to illustrate the influencing mechanism of $Na^+$ modification on the thermal expansibility of vermiculite.

## 2. Experimental

### 2.1 Modified vermiculite sample preparation

Raw vermiculite (Raw-V) samples with an average size of 1–2 mm and a thickness of 0.21–0.45 mm were collected from Yuli, China. Before modification, the Raw-V samples were

*School of Resources, Environment and Materials, Guangxi University, Nanning 530004, PR China. E-mail: goldminer@sina.com*

washed thrice using deionized water, and then dried at 60 °C for 48 h. The modification process was first conducted by adding 30 g of vermiculite into a 250 mL flask containing 150 mL of 0.5 mol $L^{-1}$ NaCl solution. After an ultrasonic treatment for 30 min and mechanical shaking for 8 h, the samples were added into a new NaCl solution and allowed to stand for 12 h. The same process was repeated twice. Then, the samples were washed using deionized water and dried at 60 °C for 48 h. Finally, the $Na^+$-modified vermiculite (Na-V) samples were successfully prepared.

### 2.2 Vermiculite's thermal expansion experiment

In this study, vermiculite's thermal expansion experiment was performed to investigate the effects of heating temperature and time on the expansion ratio. Raw-V and Na-V samples were heated using a muffle furnace at the temperatures of 400 °C, 500 °C, 600 °C, and 700 °C, and the heating time ranged from 10 to 480 s. The expansion ratio ($K$) was used as an index to evaluate the thermal expansibility of vermiculite samples and was calculated using the formula $K = \rho_0/\rho$, where $\rho_0$ and $\rho$ represent the bulk densities of Raw-V and Na-V samples, respectively. Bulk density could be obtained by measuring the mass and the volume of the samples.

### 2.3 Characterization methods

The chemical composition of the Raw-V and Na-V samples was determined using an X-ray fluorescence spectroscopy (XRF) instrument (ZXS primus-II, 4 kW, 60 kV, 150 mA). X-ray diffraction (XRD) patterns were recorded using a D8 Advance X-ray diffractometer (Bruker, Germany); the machine settings were 40 mA and 40 kV (Cu-K$\alpha$ radiation; $\lambda = 1.5418$ Å), $2\theta$ range 4–25°, $2\theta$ step scans of 0.1° and a counting time of 20 s per step. The thermal stability analysis was performed using a thermogravimetric-differential scanning calorimeter (Netzsch STA 449 F3) in the temperature range of 25–1000 °C, under pure $N_2$ atmosphere at the heating rate of 10 °C $min^{-1}$.

## 3. Results and discussion

### 3.1 Vermiculite's modification analysis and characterization

In the $Na^+$ modification process, ultrasonic vibration was adopted to accelerate the ion exchange. The presence of ultrasonic waves could not only increase the kinetic energy of sodium ions in solution but also break the van der Waals forces to release the interlaminar ions in vermiculite.[18,19] To understand the $Na^+$ modification effects, XRF, XRD and TG-DTA experiments were conducted to characterize the chemical and phase compositions and the thermal stability of Raw-V and Na-V samples. Table 1 lists the chemical composition of the Raw-V and Na-V samples. By comparison, it could be found that the $Na_2O$ content considerably increased by 73.83% from 1.49 to 2.59 wt%, while the CaO content relatively decreased by 73.25% from 1.72 to 0.46 wt% after the modification by the 0.5 mol $L^{-1}$ NaCl solution. In addition, the contents of MgO and $K_2O$ only showed a little change before and after the modification. The result indicated that during the modification process, sodium ions entered the vermiculite interlayer mainly through the exchange of calcium ions in vermiculite interlayers.

The XRD patterns of the Raw-V and Na-V samples are displayed in Fig. 1. The result showed that the diffusion peaks appeared in both patterns because of the effects of impurity constituents. The characteristic peaks of vermiculite, hydrobiotite, mica and phlogopite could be observed in both patterns. This was because vermiculite originated as mica, phlogopite, or hydrobiotite and was subsequently formed through the weathering or hydrothermal process. After the modification treatment, two differences were observed in the patterns. The first was that the d-spacing of the vermiculite reflection (002) increased from 1.212 nm to 1.433 nm. This change could be attributed to the decrease in the Coulomb force in vermiculite interlayers after the calcium ions were replaced by the sodium ions during the modification process. The second was that the characteristic peak intensity of the Na-V sample significantly increased due to the removal of some impurities during the modification process.

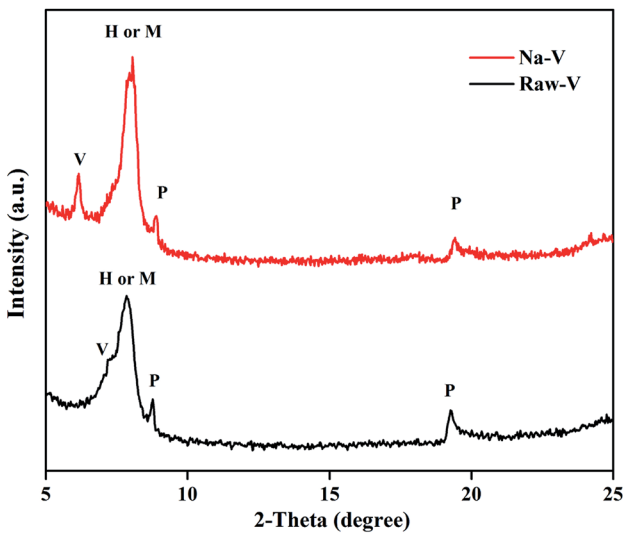


Fig. 1 XRD spectra of Raw-V and Na-V samples. (V-vermiculite, M-mica, H-hydrobiotite, and P-phlogopite).

Table 1 XRF analyses of Raw-V and Na-V samples

| | Chemical composition and contents (wt%) | | | | | | | | | |
|---|---|---|---|---|---|---|---|---|---|---|
| Sample | $SiO_2$ | MgO | $Al_2O_3$ | $Fe_2O_3$ | $K_2O$ | CaO | $TiO_2$ | $Na_2O$ | $Cr_2O_3$ | $SO_3$ |
| Raw-V | 43.40 | 24.90 | 13.60 | 6.52 | 6.16 | 1.72 | 1.64 | 1.49 | 0.22 | 0.11 |
| Na-V | 44.30 | 24.10 | 13.60 | 6.84 | 6.09 | 0.46 | 1.62 | 2.59 | 0.21 | 0.10 |

The TG-DTA analyses of the Raw-V and Na-V samples are shown in Fig. 2. According to the curves in Fig. 2a, four stages for the Raw-V sample occurred when the heating temperature increased from 25 °C to 1000 °C. The first stage occurred from 25 °C to 88 °C with a mass loss of 4.36%, which could be attributed to the removal of water molecules adsorbed on the vermiculite surface. Subsequently, the Raw-V sample underwent a second dehydration process between 88 °C and 154 °C. The mass loss of 1.03% in this stage was mainly attributed to the decomposition of some hydrates in the vermiculite interlayer. The third stage corresponded to the temperature range from 154 °C to 838 °C with a mass loss of 1.79%. According to Marcos's literature, the mass change was mainly attributed to the removal of chemical structural water in the dehydroxylation reaction. As the temperature increased to 1000 °C, the Raw-V sample underwent a mass loss of 1.49%. In this stage, the thermal decomposition reaction occurred and resulted in the formation of compounds, such as forsterite, mullite, and alumina. After the modification, the TG-DTA curve of the Na-V sample basically showed a similar trend to that of the Raw-V sample. However, there were some differences to be observed. The first two stages in Fig. 2a merged into one stage from 25 °C to 91 °C in Fig. 2b. This was because the Raw-V testing sample was not subjected to drying pretreatment, resulting in residual surface water. Compared with the interlayer water, the evaporation of surface water required less energy. Therefore, the first peak occurred at a low temperature of 88 °C. This peak disappeared in Fig. 2b because of the drying pretreatment for the Na-V testing sample. In addition, the transition point temperature in this stage decreased from 154 °C to 91 °C. The result indicated that the binding energy of the sodium ion and water molecule was relatively weak, and the dehydration reaction could occur at a lower temperature.

### 3.2 Effect of $Na^+$ modification on vermiculite's thermal expansibility

Fig. 3 shows the effects of the heating temperature and time on the expansion ratios of the Raw-V and Na-V samples. It could be observed that the expansion ratio increased with the increasing in heating temperature. The expansion ratio of the Raw-V sample was only 2.42 at 400 °C for 180 s. It indicated that the interlaminar vapour pressure was insufficient to cause vermiculite's exfoliation at lower temperatures. When the temperature increased to 700 °C, the expansion ratio reached up to 6.95. The Na-V sample showed a similar trend to that of the Raw-V sample under the same conditions. The result indicated that the heating temperature was a major factor affecting the expansion behaviors of vermiculite. In addition, the curves in Fig. 3 could be divided into two stages with the change of heating time. The first is the sharp expansion stage due to the flash evaporation of interlayer water. When the water evaporation was completed, vermiculite had almost no volume change and entered the second stage of expansion equilibration. The higher the heating temperature, the shorter the time to reach the expansion equilibration. For the Raw-V sample, the equilibration time needed about 300 s at the heating temperature of 400 °C. When the temperature increased to 700 °C, it took only 60 s to achieve the expansion equilibration. After the modification treatment, two differences were observed in the curves. The first was that the Na-V sample could achieve a larger expansion ratio than that of the Raw-V sample under the same conditions. At the heating temperatures of 400 °C, 500 °C, 600 °C, and 700 °C, the expansion ratios of the Na-V sample in the equilibration stage increased by 22.5%, 26.5%, 22.3%, and 10.9%, respectively, compared with those of the Raw-V sample. The second was that the $Na^+$ modification could obviously shorten the equilibration time. That is to say that the Na-V sample needed less energy to achieve the same expansion ratio compared to the Raw-V sample. The results could be attributed to the changes in interlayer water content and the binding energy between the interlayer ion and water molecule after the $Na^+$ modification.

### 3.3 $Na^+$ modification influencing the mechanisms of vermiculite's expansibility

As we know, the thermal expansion of vermiculite is attributed to the rapid evaporation of interlayer water during flash-heating. Therefore, both the interlayer water content and the binding state of the interlayer ion and water molecule will affect the

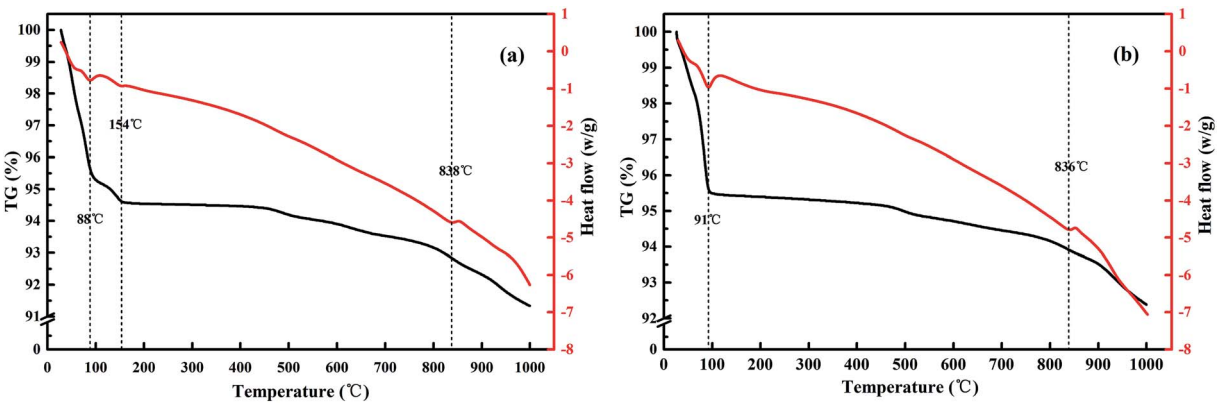


Fig. 2 TG-DTA analyses of Raw-V (a) and Na-V (b) samples.

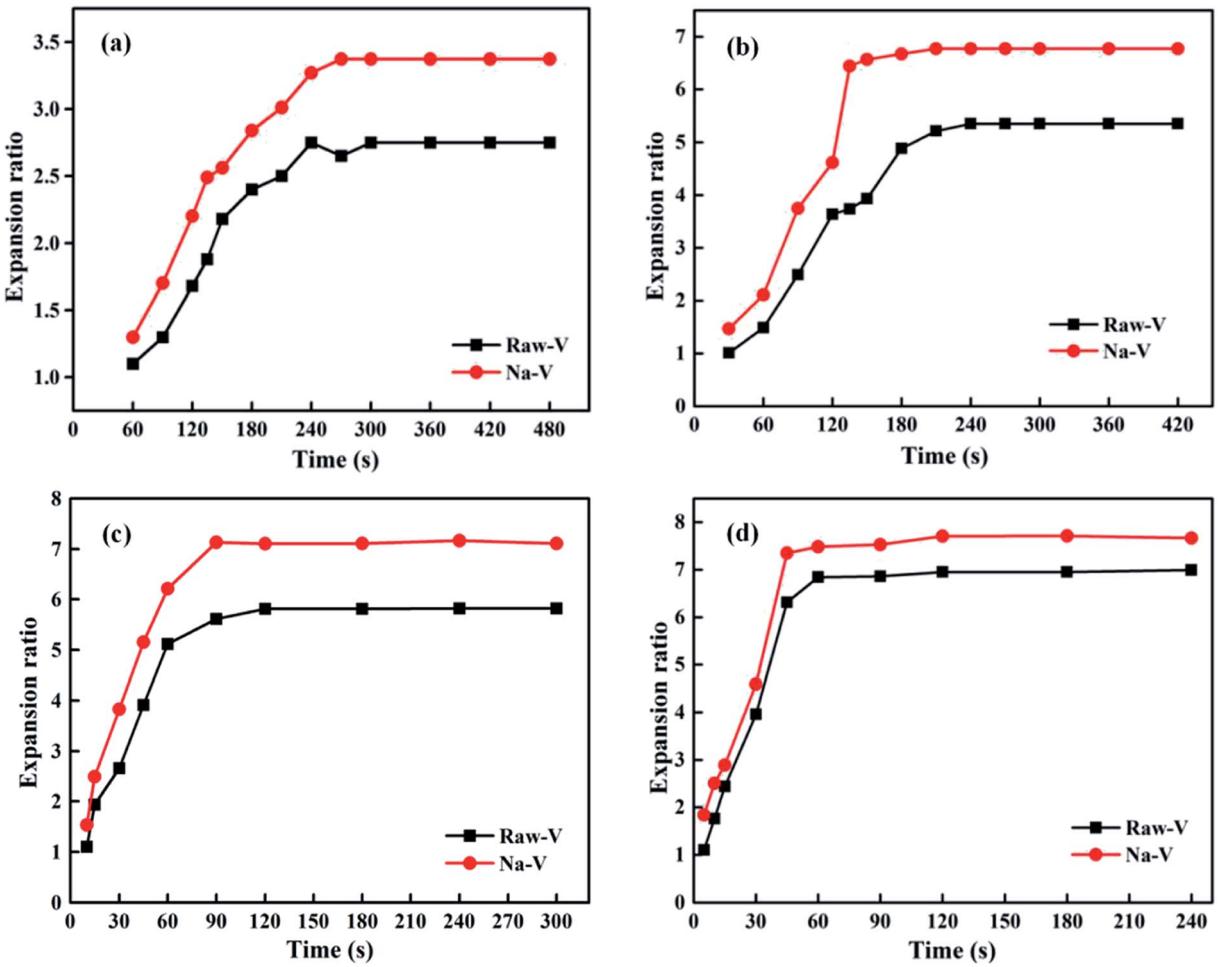


Fig. 3 Effect of heating time on the expansion ratio at various temperatures. (a) 400 °C, (b) 500 °C, (c) 600 °C, and (d) 700 °C.

thermal expansibility of vermiculites. The aforementioned analyses of TG-DTA indicated that the existing status of the interlayer water in vermiculite showed three forms, including free water, bound water, and structural water. When the sample was exposed to the ambient environment, the water molecule in the air was absorbed by vermiculite flakes under the surface forces. Therefore, the free water content was determined by ambient humidity and surface properties of vermiculite layers. As for bound water, because of the existence of interlayer ions, the water molecules were combined to form hydrated ions in vermiculite interlayers. Thus, the interlayer ion type is a crucial factor for the bound water content. In addition, the binding force of the interlayer ion and the water molecule determined the energy consumption of the thermal expansion of vermiculite. Structural water is defined as the water present in the vermiculite lattice in the form of hydroxy groups, which is mainly related to the geological process of vermiculite formation. Based on the analysis mentioned above, the reason could be well illustrated that the vermiculite samples from various origins exhibited different expansion behaviors under the same conditions. In this study, the essence of the $Na^+$ modification to improve vermiculite thermal expansibility was the changes in the bound water content and the binding energy of the hydrated ion.

**3.3.1. Coordination simulation based on the molecular dynamics model.** XRF analysis showed that during the modification process, sodium ions entered the vermiculite interlayer mainly through the exchange of calcium ions in vermiculite interlayers. Aimed at illustrating the interactions of the interlamellar ion and the water molecule, a molecular dynamics model was developed using the software of Material Studio. Because $Na^+$ and $Ca^{2+}$ have different coordination abilities with water molecules, the structural formulas of hydrated ions can be written as $[Na(H_2O)_n]^+$ and $[Ca(H_2O)_n]^{2+}$, respectively. The convergence criteria for structure optimization and energy calculation were set as energy tolerance of $2.0 \times 10^{-5}$ eV per atom, maximum force tolerance of 0.1 eV $Å^{-1}$, and maximum displacement tolerance of 0.3 Å.

In this model, the coordination bond length was calculated to evaluate the binding ability between the hydrated ion and the water molecule. The shorter the bond length, the stronger the binding force. When the bond length increases to a value that is larger than the sum of the two radii,[20] the repulsive interactions occur, and the binding interactions disappear. Fig. 4 shows the configurations of hydrated sodium ions with various coordination numbers of water molecules. The result indicated that

 

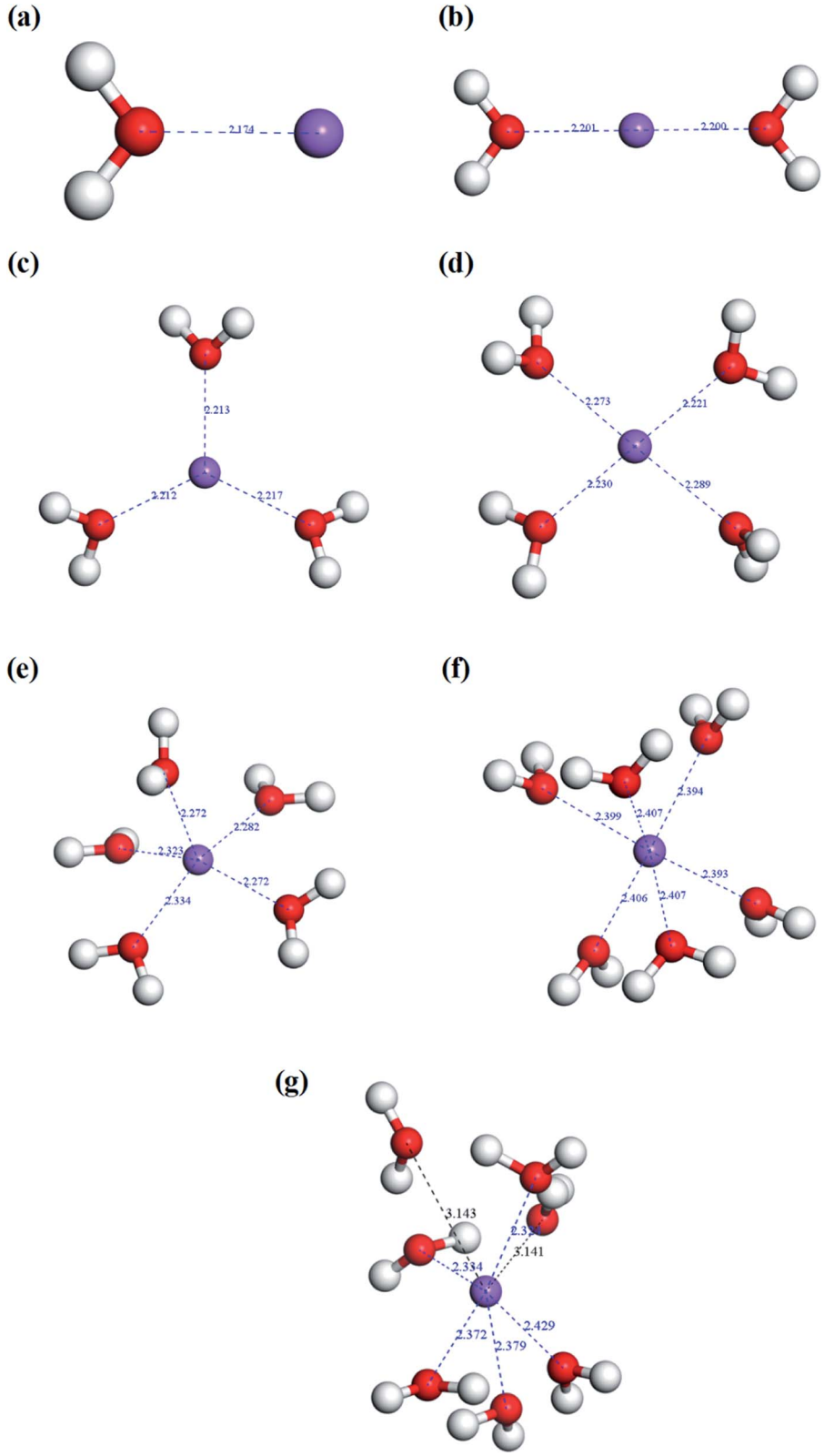


Fig. 4 Coordination simulation of hydrated sodium ions with different water molecules. (a) $Na[H_2O]^+$, (b) $Na[H_2O]_2^+$, (c) $Na[H_2O]_3^+$, (d) $Na[H_2O]_4^+$, (e) $Na[H_2O]_5^+$, (f) $Na[H_2O]_6^+$, and (g) $Na[H_2O]_7^+$.

the bond length increased with an increase in the coordination number. In Fig. 4a, the bond length is only 2.174 Å for a one-coordinate hydrated sodium ion. When the coordination number increased to six, the largest bond length came up to 2.407 Å. However, as the coordination number continued to increase, some bond lengths began to surpass the value of 2.640

Å. In Fig. 4g, the largest bond length reached up to 3.143 Å. It means that the configuration was unstable due to the weak binding force. Therefore, the maximum coordination number for the hydrated sodium ion is six. Fig. 5 shows the configurations of hydrated calcium ions with different coordination numbers of water molecules. The simulation result presented

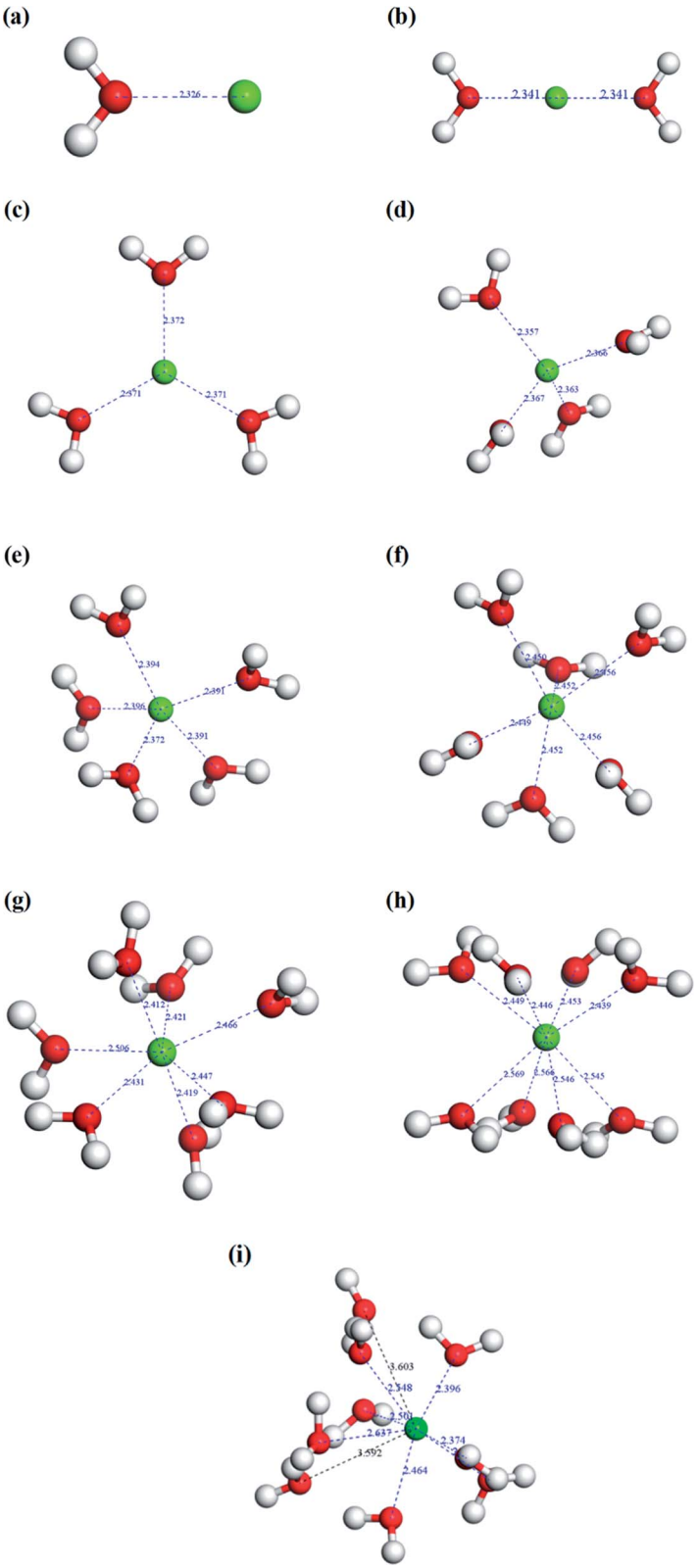


Fig. 5 Coordination simulation of hydrated calcium ions with different water molecules. (a) $Ca[H_2O]^{2+}$, (b) $Ca[H_2O]_2^{2+}$, (c) $Ca[H_2O]_3^{2+}$, (d) $Ca[H_2O]_4^{2+}$, (e) $Ca[H_2O]_5^{2+}$, (f) $Ca[H_2O]_6^{2+}$, (g) $Ca[H_2O]_7^{2+}$, (h) $Ca[H_2O]_8^{2+}$, and (i) $Ca[H_2O]_9^{2+}$.

 

a similar trend where the bond length was proportional to the coordination number. In Fig. 5a, when the calcium ion is coordinated with one water molecule, a strong interaction appeared with a short bond length of only 2.326 Å. When the coordination number increased to eight, the largest bond length in this configuration reached up to 2.569 Å. As the coordination number continued to increase, some bond lengths began to exceed the value of 2.700 Å.[21] Just as shown in Fig. 5i, the largest bond length came up to 3.603 Å in the nine-coordinate structure. It means that the maximum coordination number for the hydrated calcium ion is eight. According to the charge conservation law, a divalent calcium ion was replaced by two monovalent sodium ions during the ion exchange process. Therefore, the $Na^+$ modification can significantly improve the interlayer water content of vermiculite, and the modified vermiculite can correspondingly achieve a high expansion ratio.

**3.3.2. Calculations of the binding energy and dehydration enthalpy change.** In the expansion experiment, it was observed that the Raw-V and Na-V samples presented different thermal expansibilities under the same conditions. In addition to the influence of the interlayer water content, the binding force between the interlayer ion and water molecule also played a significant role in the expansion performance of vermiculite. Aimed at evaluating the binding ability, the binding energy (BE) and the dehydration enthalpy change ($\Delta H$) were respectively calculated to compare the stability of hydrated sodium and calcium ions with various coordination numbers.

Here, BE is defined as the coordination energy between the central ion and the water molecules. Based on the energy conservation law, BE can be derived through eqn (1), where $E_{total}$ represents the crystal configuration energy, $E_{H_2O}$ is the energy of all water molecules, and $E_m$ is the energy of $Na^+$ or $Ca^{2+}$.

$$BE = E_{total} - E_{H_2O} - E_m \quad (1)$$

Based on the results of the molecular dynamics simulation, the maximum coordination number for hydrated sodium and calcium ions are six and eight, respectively. Fig. 6 depicts the relationship between BE and the coordination number. The results showed that the absolute BE values of the hydrated sodium ion were always higher than those of the hydrated calcium ion. When the coordination number was six, the absolute BE values were 123.67 and 264.59 kcal $mol^{-1}$, respectively. The result indicated that the binding energy of $Na^+$ and $H_2O$ is weaker than that of $Ca^{2+}$ and $H_2O$. Alternatively, after the modification, the Na-V sample needed less energy in the dehydration process. The calculation results satisfactorily explained the reason why the Na-V sample could achieve a higher expansion ratio under a comparatively low heating temperature.

For validating the BE calculation results, the enthalpy change ($\Delta H$) of the dehydration reaction was calculated according to eqn (2), where $H_n$ and $H_{n-1}$ represent the enthalpies of hydrated ions with $n$ and $n-1$ coordination, respectively, and $H_{H_2O}$ represents the enthalpy of one water molecule.

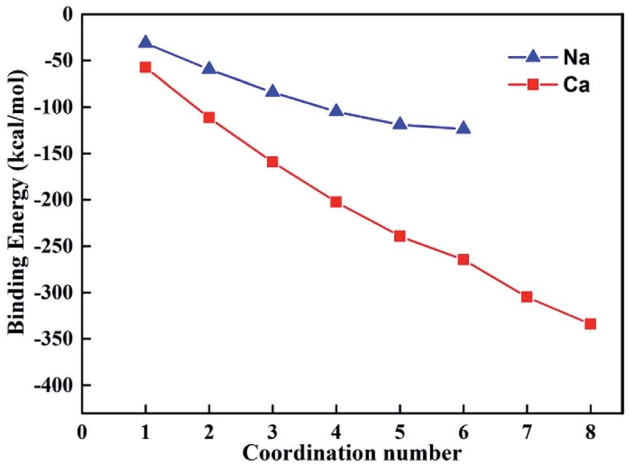


Fig. 6 Effects of the coordination number on the binding energy.

$$\Delta H = H_{n-1} + H_{H_2O} - H_n \quad (2)$$

The dehydration reaction formula of hydrated sodium and calcium ions can be written as follows:

$$Na(H_2O)_n^{+} \xrightarrow{\text{hydration}} Na(H_2O)_{n-1}^{+} + H_2O$$

$$Ca(H_2O)_n^{2+} \xrightarrow{\text{hydration}} Ca(H_2O)_{n-1}^{2+} + H_2O$$

Fig. 7 shows the dehydration enthalpy changes in hydrated sodium and calcium ions with different coordination numbers. It could be found that the dehydration reaction was endothermic, and the enthalpy change decreased with the increase in the coordination number, which was mainly attributed to the decrease in binding energy between the interlayer ion and water molecule. When the sodium ion was coordinated with one water molecule, the dehydration enthalpy change was 31.21 kcal $mol^{-1}$. As the coordination number increased to six,

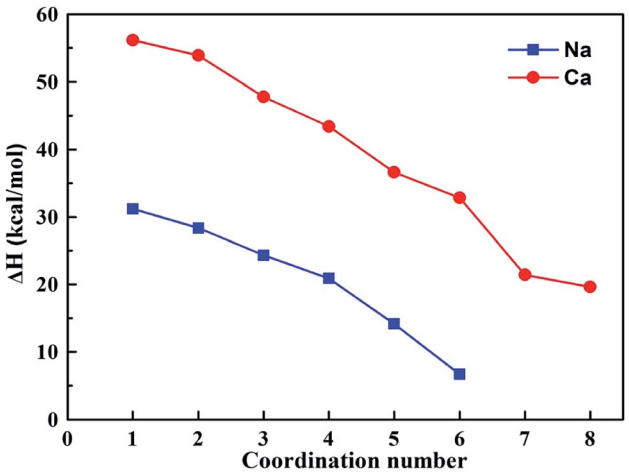


Fig. 7 Effect of the coordination number on the dehydration enthalpy changes.

the removal of one water molecule from the hexahydrate sodium ion only needed 6.7 kcal $mol^{-1}$. The dehydration enthalpy change of the hydrated calcium ion showed a similar trend to that of the hydrated sodium ion. In addition, by comparing the curves in Fig. 7, it could be observed that the dehydration enthalpy change of the hydrated sodium ion was always lower than that of the hydrated calcium ion. For monohydrate and hexahydrate, the dehydration enthalpy changes dropped by 44.43% and 79.58%, respectively, after the modification. Therefore, the calculation results well demonstrated the influencing mechanism of the $Na^+$ modification on the thermal expansibility of vermiculite.

## 4. Conclusion

$Na^+$ modification could significantly improve the expansion performance of vermiculite at the temperatures of 400–700 °C. The essence of the modification was the replacement of interlamellar calcium ions by sodium ions through ion exchange. Based on the molecular dynamics simulation, $Na^+$ modification could improve the interlayer water content by the hydration reaction. The vermiculite exfoliation was influenced by the interlayer vapour pressure, which was generated through the thermal evaporation of interlayer water. In addition, the calculation results of the binding energy and dehydration enthalpy change indicated that the binding energy of the sodium ion and water molecule is weaker than that of the calcium ion and the water molecule, and the dehydration reaction of the hydrated sodium ion needs less energy than that of the hydrated calcium ion. The simulation and calculation results showed a good agreement with vermiculite thermal expansion experiments. This study provides a novel method for the preparation of high-performance expanded vermiculite.

## Conflicts of interest

There are no conflicts to declare.

## Acknowledgements

This work was financially supported by National Natural Science Foundation of China (No. 51974095), Natural Science Foundation of Guangxi Province (No. 2018GXNSFAA138166) and College Student's Innovation and Entrepreneurship Training Program of Guangxi University (201810593215).

## References

1 J. Chen, C. Zhou, S. Wang and S. Li, Impacts of energy consumption structure, energy intensity, economic growth, urbanization on $PM_{2.5}$ concentrations in countries globally, *Appl. Energy*, 2018, **230**, 94–105.
2 C. Duan and B. Chen, Analysis of global energy consumption inequality by using Lorenz curve, *Energy Procedia*, 2018, **152**, 750–755.
3 Y. Hu, L. Peng, X. Li, X. Yao, H. Bin and T. Chi, A novel evolution tree for analyzing the global energy consumption structure, *Energy*, 2018, **147**, 1177–1187.
4 G. F. Walker, *Vermiculites and some related mixed-layer minerals*, Mineralogical Society, London, 1951.
5 A. Argüelles, M. Leoni, J. A. Blanco and C. Marcos, Semi-ordered crystalline structure of the Santa Olalla vermiculite inferred from X-ray powder diffraction, *Am. Mineral.*, 2010, **95**, 126–134.
6 V. I. Andronova, A study of the crystalline structure of vermiculite from the Tebinbulak deposit, *Refract. Ind. Ceram.*, 2007, **48**, 91–95.
7 S. Hillier, E. M. M. Marwa and C. M. Rice, On the mechanism of exfoliation of 'Vermiculite', *Clay Miner.*, 2013, **48**, 563–582.
8 J. Addison, Vermiculite: a review of the mineralogy and health effects of vermiculite exploitation, *Regul. Toxicol. Pharmacol.*, 1995, **21**, 397–405.
9 J. Kariya, J. Ryu and Y. Kato, Development of thermal storage material using vermiculite and calcium hydroxide, *Appl. Therm. Eng.*, 2016, **94**, 186–192.
10 M. Sutcu, Influence of expanded vermiculite on physical properties and thermal conductivity of clay bricks, *Ceram. Int.*, 2015, **41**, 2819–2827.
11 F. Zhou, H. Zhi and C. Wang, Preparation and microstructure of in-situ gel modified expanded vermiculite, *Ceram. Int.*, 2013, **39**, 4075–4079.
12 Y. El Mouzdahir, A. Elmchaouri, R. Mahboub, A. Gil and S. A. Korili, Synthesis of nano-layered vermiculite of low density by thermal treatment, *Powder Technol.*, 2009, **189**, 2–5.
13 E. M. M. Marwa, C. M. Rice and A. A. Meharg, The effect of heating temperature on the properties of vermiculites from Tanzania with respect to potential agronomic applications, *Appl. Clay Sci.*, 2016, **43**, 376–382.
14 A. Justo, C. Maqueda, J. L. Perez-Rodriguez and E. Morillo, Expansibility of some vermiculites, *Appl. Clay Sci.*, 1989, **4**, 509–519.
15 C. Marcos and I. Rodriguez, Expansion behaviour of commercial vermiculites at 1000 °C, *Appl. Clay Sci.*, 2010, **48**, 492–498.
16 C. Marcos and I. Rodriguez, Expansibility of vermiculites irradiated with microwaves, *Appl. Clay Sci.*, 2011, **51**, 33–37.
17 C. Marcos and I. Rodriguez, Effect of propanol and butanol and subsequent microwave irradiation on the structure of commercial vermiculites, *Appl. Clay Sci.*, 2017, **144**, 104–114.
18 E. B. Flint and K. S. Suslick, The temperature of cavitation, *Science*, 1991, **253**, 1397–1399.
19 K. S. Suslick and G. J. Price, Applications of ultrasound to material chemistry, *Annu. Rev. Mater. Sci.*, 1999, **29**, 295–326.
20 P. Linus, *The Nature of the Chemical Bond and the Structure of Molecules and Crystals*, Cornell University Press, New-York, 1960.
21 A. K. Katz, J. P. Glusker, S. A. Beebe and C. W. Bock, Calcium Ion Coordination: A Comparison with That of Beryllium, Magnesium, and Zinc, *J. Am. Chem. Soc.*, 1996, **118**, 5752–5763.

 